

Control Framework for Slung Load Transportation with Two Aerial Vehicles

Pedro O. Pereira and Dimos V. Dimarogonas

Abstract

We model a point mass load tethered to two aerial vehicles, and propose a control strategy that guarantees that the load tracks a desired position trajectory. Our framework consists in designing an input and a state transformation which converts the quadrotors-load system into three decoupled subsystems: one concerning the position of the load, with dynamics similar to those of an under-actuated aerial vehicle; one concerning the angle between the cables, with double integrator dynamics; and another concerning the yaw motion of the plane formed by the cables, also with double integrator dynamics. Once the decoupling is done, controllers from the literature can be leveraged, which we take advantage of when controlling the subsystem with dynamics similar to those of an under-actuated aerial vehicle. Simulations are presented which validate the proposed algorithm.

I. INTRODUCTION

Execution of complex manipulation tasks with aerial vehicles is an active topic of research in robotics. Compared to ground robots, aerial robots allow for manipulation tasks to be executed in difficult to access spaces, paving the way to new applications, such as the inspection and maintenance of aging infrastructures [1].

Multi-rotor helicopters have been used to perform complex autonomous tasks [2], including manipulation tasks with grippers, robotic arms and cables [3]–[10]. Autonomy is usually achieved with the help of vision [11]–[13], and stability of control laws may be extended when a load is attached to the aerial vehicle [14]. Quadrotors, in particular, are preferred to others types of UAVs owing to their capability to hover, to take off and land vertically, to their high manoeuvrability, and to the availability of inexpensive components.

In this manuscript, we focus on the problem of transporting a load in a system composed of one load and two quadrotors, and where each quadrotor is connected to the load by a cable of fixed length. Grippers and robotic arms, when compared to cables, are expensive and mechanically complex, which motivates the study of tethered transportation. Moreover, transportation with multiple aerial vehicles adds robustness for when one or more team members suffers a failure, such as an actuator failure [3]. A model of this system, also referred to as slung load system, is found in [15], and controllers for position trajectory tracking of the load are found in the literature [8], [16], [16]–[21]. Controllers for helicopters with experimental validation are found in [16], [17], where vision was used to estimate the state used in the feedback loop. For quadrotors, controllers are found in [8], [18]–[22], which explore differential flatness for planning trajectories for the transporting quadrotors and which minimize sway; or which explore the dynamics to design controllers based on Lyapunov methods, such as backstepping. Adaptive strategies that compensate for the presence of unmodeled or unknown parameters, such as the load's mass or the cables lengths, are also found [23], [24].

In this paper, we propose a control framework for trajectory tracking of the load. While in the literature specific control laws are found [3], [16], [21], we instead provide a general framework that transforms the quadrotors-load system into three decoupled subsystems, for which controllers are found in the literature. One of the subsystems, concerning the load's position, has the dynamics of an under-actuated aerial vehicle. In particular, we provide a throttle control law which allows us to leverage hierarchical controllers for VTOL vehicles [25], and which constitutes one of the paper's contributions. The other two subsystems, concerning the angle between the cables and the yaw position of the plane formed by the cables, have the dynamics of double integrators, for which controllers are also found in the literature. One of the control design challenges relates to the fact that a continuous controller defined over the whole state space cannot be found (for example, not defined when the cables overlap). One of the paper's contributions is to make explicit the domain where the control strategy is defined, and to provide specific control laws that guarantee that a solution never exits that domain.

The remainder of this paper is structured as follows. In Section III, we describe the system's dynamics and present the problem statement. In Section IV, we present and explain the design steps for the controller that transforms the system into the three decoupled subsystems. In Section V, we propose specific controllers for those subsystems. In Section VI, we consider the UAVs attitude inner loop. Finally, in Section VII, we provide simulations which illustrate the proposed algorithm in action.

II. NOTATION

The map $\mathcal{S} : \mathbb{R}^3 \ni x \mapsto \mathcal{S}(x) \in \mathbb{R}^{3 \times 3}$ yields a skew-symmetric matrix and it satisfies $\mathcal{S}(a)b := a \times b$, for any $a, b \in \mathbb{R}^3$. $\mathbb{S}^2 := \{x \in \mathbb{R}^3 : x^T x = 1\}$ denotes the set of unit vectors in \mathbb{R}^3 . The map $\Pi : \mathbb{S}^2 \ni x \mapsto \Pi(x) := I_3 - xx^T \in \mathbb{R}^{3 \times 3}$ yields a matrix that represents the orthogonal projection onto the subspace perpendicular to $x \in \mathbb{S}^2$. We denote by $e_1, \dots, e_n \in \mathbb{R}^n$

and with the kinematics given by

$$Z_k(z_d) := z_d = \begin{bmatrix} v \\ v_1 \\ v_2 \end{bmatrix} \left(= \begin{bmatrix} \dot{p} \\ \dot{p}_1 \\ \dot{p}_2 \end{bmatrix} \right), \quad (7)$$

and the dynamics given by

$$Z_d(z, u) := \begin{bmatrix} \sum_{i \in \{1,2\}} \frac{T_i(z, u)}{m} n_i(z) - g e_3 \\ \frac{u_1}{m_1} - \frac{T_1(z, u)}{m_1} n_1(z) - g e_3 \\ \frac{u_2}{m_2} - \frac{T_2(z, u)}{m_2} n_2(z) - g e_3 \end{bmatrix} \left(= \begin{bmatrix} \dot{v} \\ \dot{v}_1 \\ \dot{v}_2 \end{bmatrix} \right), \quad (8)$$

where g stands for the acceleration due to gravity. The accelerations in (8) are written based the Newton's equation of motion, considering the net force on each point mass illustrated in Fig. 1. However, the latter equations do not provide any insight about the tensions T_1 and T_2 in Fig. 1, since they are internal forces. The constraint that any trajectory of (5) must be contained in \mathbb{Z} , enforces the vector field (6) to be in the tangent set (3). This constraint uniquely defines the tensions, i.e., for any $(z, u) \in \mathbb{Z} \times \mathbb{R}^6$, it follows that

$$\begin{aligned} Z(z, u) \in T_z \mathbb{Z} \Rightarrow \\ \Rightarrow \begin{bmatrix} T_1(z, u) \\ T_2(z, u) \end{bmatrix} = \underbrace{\begin{bmatrix} \frac{m}{m_1} + 1 & \cos(\theta) \\ \cos(\theta) & \frac{m}{m_2} + 1 \end{bmatrix}^{-1} \left(\begin{bmatrix} \frac{m}{m_1} n_1(z_k)^T & 0_{1 \times 3} \\ 0_{1 \times 3} & \frac{m}{m_2} n_2(z_k)^T \end{bmatrix} \begin{bmatrix} u_1 \\ u_2 \end{bmatrix} + m \begin{bmatrix} \frac{\|v_1 - v\|^2}{l_1} \\ \frac{\|v_2 - v\|^2}{l_2} \end{bmatrix} \right)}_{=: M_T(z_k) \in \mathbb{R}^{2 \times 6}} \Big|_{\cos(\theta) = n_1(z_k)^T n_2(z_k)}. \end{aligned} \quad (9)$$

The vector field (6) may also be derived by means of the Euler-Lagrange formalism [19]. Notice that the quadrotors-load system has a 7th dimensional generalized coordinate (three coordinates for the load's position, and two coordinates for each cable unit vector), while the input to the system is only 6th dimensional. That means that the quadrotors-load system is under-actuated. Let us now state the problem to be solved in this paper.

Problem 1: Given a desired smooth position trajectory $p^* \in \mathbb{R}_{\geq 0} \mapsto \mathbb{R}^3$, design $u = (u_1, u_2) : \mathbb{R}_{\geq 0} \mapsto \mathbb{R}^6$ such that $\lim_{t \rightarrow \infty} (p(t) - p^*(t)) = 0$ along trajectories of (5).

We emphasize that the vector field (6) is input affine. In fact,

$$Z(z, u) = A(z) + \begin{bmatrix} 0_{9 \times 6} \\ B(z_k) \end{bmatrix} \begin{bmatrix} u_1 \\ u_2 \end{bmatrix},$$

where $A(z) := Z(z, 0_6) \in \mathbb{R}^{18}$ and

$$B(z_k) := \begin{bmatrix} \frac{1}{m} \sum_{i \in \{1,2\}} n_i(z_k) e_i^T M_T(z_k) \\ \frac{1}{m_1} ([I_3 \ 0_{3 \times 3}] - n_1(z_k) e_1^T M_T(z_k)) \\ \frac{1}{m_2} ([0_{3 \times 3} \ I_3] - n_2(z_k) e_2^T M_T(z_k)) \end{bmatrix} \in \mathbb{R}^{9 \times 6}, \quad (10)$$

with M_T as in (9), $e_1 = (1, 0)$ and $e_2 = (0, 1) \in \mathbb{S}^1$. We emphasize that B in (10) depends exclusively on the kinematic variables (which is particularly important in what follows).

IV. CONTROL LAW DESIGN

A. Control Strategy

Let us explain the pursued control strategy, which is illustrated in Fig. 2. As a first step, we introduce an input transformation from $\nu := (\nu_1, \nu_2, \nu_3) \in \mathbb{R}^{4+1+1}$ to $u \in \mathbb{R}^6$. Intuitively, $\nu_1 := (T, \tau) \in \mathbb{R}^{1+3}$ where T will stand for the force along the direction of N in Fig. 1, while τ will stand for the angular acceleration of the unit vector associated to N ; and we design ν_1 to control the position of the load. On the the other hand, $\nu_2 \equiv \tau_\theta \in \mathbb{R}$ will stand for the acceleration of the angle between the cables (θ in Fig. 1), and we will design ν_2 to control that angle. And, finally, $\nu_3 \equiv \tau_\psi \in \mathbb{R}$ will stand for the acceleration of the yaw position associated to the plane formed by the two cables, and we will design ν_3 to control that yaw position. The idea is that $\nu := (\nu_1, \nu_2, \nu_3)$ provides a more meaningful input to design, and once it is designed, one can map ν to u (the actual input) by means of the function \bar{u} (see Fig. 2). This is done in Section IV-C.

In the second step, done in Section IV-D, we provide a coordinate transformation g that maps a $z \in \tilde{\mathbb{Z}} \subset \mathbb{Z}$ into an $x \in \tilde{\mathbb{X}}$ (g , $\tilde{\mathbb{Z}}$ and $\tilde{\mathbb{X}}$ are defined later), and with this coordinate transformation, we obtain a new vector field, which comes from the composition of the state transformation with the vector field Z in (6) and the input transformation. In fact, this new vector field is composed of three decouple vector fields, namely X_1 , X_2 and X_3 , where each vector field has as an input ν_1 , ν_2 and ν_3 , respectively (see Fig. 2). The benefit of this coordinate transformation is that it highlights the decoupled structure of the problem, and thus it allows us to design control laws for ν_1 , ν_2 and ν_3 separately. One of our main contributions is to show that the vector field X_1 is one for which controllers already exist in the literature.

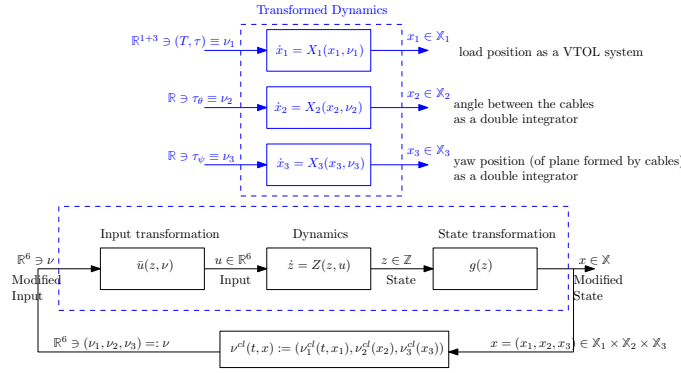


Fig. 2: Control strategy: the vector field (6) is decomposed into three decoupled vector fields, by means of an input and state transformation.

In the final step, done in Section V, we present control laws $\mathbb{R}_{\geq 0} \times \tilde{\mathbb{X}}_1 \ni (t, x_1) \mapsto \nu_1^{cl}(t, x_1) \in \mathbb{R}^4$, $\tilde{\mathbb{X}}_2 \ni x_2 \mapsto \nu_2^{cl}(x_2) \in \mathbb{R}$ and $\tilde{\mathbb{X}}_3 \ni x_3 \mapsto \nu_3^{cl}(x_3) \in \mathbb{R}$ and combine them to define $\tilde{\mathbb{X}} := \tilde{\mathbb{X}}_1 \times \tilde{\mathbb{X}}_2 \times \tilde{\mathbb{X}}_3$ and $\mathbb{R}_{\geq 0} \times \tilde{\mathbb{X}} \ni (t, x) \mapsto \nu^{cl}(t, x) \in \mathbb{R}^6$ as

$$\nu^{cl}(t, x) := (\nu_1^{cl}(t, x_1), \nu_2^{cl}(x_2), \nu_3^{cl}(x_3)) \quad (11)$$

that guarantees that Problem 1 is accomplished and that $\tilde{\mathbb{X}}$ is positively invariant. Using the mapping \bar{u} , one constructs the control law for the original system, i.e., $\mathbb{R}_{\geq 0} \times \tilde{\mathbb{Z}} \ni (t, z) \mapsto u^{cl}(t, z) \in \mathbb{R}^6$ defined as

$$u^{cl}(t, z) := \bar{u}(z, \nu^{cl}(t, x))|_{x=g(t, z)}, \quad (12)$$

which yields the closed loop vector field

$$\mathbb{R}_{\geq 0} \times \tilde{\mathbb{Z}} \ni (t, z) \mapsto Z^{cl}(t, z) := Z(z, u^{cl}(t, z)) \in \mathbb{R}^{18}. \quad (13)$$

One of the challenges in the control design is to guarantee that a solution $t \mapsto z(t)$ of $\dot{z}(t) = Z^{cl}(t, z(t))$ remains in $\{z \in \tilde{\mathbb{Z}} : g(z) \in \tilde{\mathbb{X}}\} \subset \tilde{\mathbb{Z}} \subset \mathbb{Z}$ which is the set where the control law (12) is well defined.

B. Preliminary Definitions

We are interested in controlling the position of the load, the angle between the cables and the yaw position of the plane defined by the cables, where we emphasize that these quantities depend exclusively on the kinematic variables ($z_k := (p, p_1, p_2) \in \mathbb{Z}_k$). With that in mind, and in order to construct the input and coordinate transformation illustrated in Fig 2, we must define the first and second derivatives of smooth functions in \mathbb{Z}_k , or, more generally, in a subset of \mathbb{Z}_k which we will name $\tilde{\mathbb{Z}}_k$ (with that in mind, define $\tilde{\mathbb{Z}} := \{(z_k, z_d) \in \mathbb{Z} : z_k \in \tilde{\mathbb{Z}}_k\} \subset \mathbb{Z}$). Consider then a smooth function $f : \tilde{\mathbb{Z}}_k \ni z_k \mapsto f(z_k) \in \mathbb{R}^n$ for some $n \in \mathbb{N}$. We introduce

$$\begin{aligned} f^{(1)} : \tilde{\mathbb{Z}} \ni (z_k, z_d) &\mapsto f^{(1)}(z_k, z_d) (= \dot{f}(z_k)) \in \mathbb{R}^n, \\ f^{(2)} : \tilde{\mathbb{Z}} \times \mathbb{R}^6 \ni (z, u) &\mapsto f^{(2)}(z, u) (= \ddot{f}(z_k)) \in \mathbb{R}^n, \end{aligned}$$

as the first and second derivative of f along the vector field (6). These are therefore defined as

$$f^{(1)}(z_k, z_d) := Df(z_k)Z_k(z_d) \stackrel{(\gamma)}{=} Df(z_k)z_d, \quad (14)$$

and

$$\begin{aligned} f^{(2)}(z, u) &:= D_1 f^{(1)}(z_k, z_d)Z_k(z_d) + D_2 f^{(1)}(z_k, z_d)Z_d(z, u) \\ &\stackrel{(14)}{=} D_1 f^{(1)}(z_k, z_d)Z_k(z_d) + Df(z_k)Z_d(z, u) \\ &\stackrel{(14)}{=} \underbrace{D_1 f^{(1)}(z_k, z_d)z_d + Df(z_k)Z_d(z, 0_6)}_{=: A_f(z) \in \mathbb{R}^{n \times 6}} + \underbrace{Df(z_k)B(z_k)}_{=: B_f(z_k) \in \mathbb{R}^{n \times 6}} u. \end{aligned} \quad (15)$$

Proposition 1: Let $p, v, a : \mathbb{R} \mapsto \mathbb{R}^3$ (with $p(\cdot) \neq 0_3$), where $(\dot{p}(t), \dot{v}(t)) = (v(t), a(t))$ for all $t \in \mathbb{R}$. Then, for

$$\begin{aligned} \mathbb{R}^3 \setminus \{0_3\} \ni p &\mapsto n(p) := \frac{p}{\|p\|} \in \mathbb{S}^2, \\ (\mathbb{R}^3 \setminus \{0_3\}) \times \mathbb{R}^3 \ni (p, v) &\mapsto \omega(p, v) := \mathcal{S}(n(p)) \frac{v}{\|p\|} \in T_{n(p)} \mathbb{S}^2, \\ (\mathbb{R}^3 \setminus \{0_3\}) \times \mathbb{R}^3 \times \mathbb{R}^3 \ni (p, v, a) &\mapsto \tau(p, v, a) := \mathcal{S}(n(p)) \left(\frac{a}{\|p\|} - 2 \frac{v}{\|p\|} \frac{v^T}{\|p\|} n(p) \right) \in T_{n(p)} \mathbb{S}^2, \end{aligned} \quad (16)$$

it holds that $\dot{n}(p(t)) = \mathcal{S}(\omega(p(t), v(t))) n(p(t))$ and that $\dot{\omega}(p(t), v(t)) = \tau(p(t), v(t), a(t))$, for all $t \in \mathbb{R}$. The proof follows from straightforward calculations.

With Proposition 1 in mind, suppose now that $f : \tilde{\mathbb{Z}}_k \in z_k \mapsto f(z_k) \in \mathbb{R}^3 \setminus \{0_3\}$. We can then define

$$n_f : \tilde{\mathbb{Z}}_k \ni z_k \mapsto n_f(z_k) := n(f(z_k)) \in \mathbb{S}^2, \quad (17)$$

$$\begin{aligned} \omega_f : \tilde{\mathbb{Z}} \ni (z_k, z_d) &\mapsto \omega_f(z_k, z_d) := \omega(f(z_k), f^{(1)}(z_k, z_d)) \in \mathbb{R}^3, \\ \tau_f : \tilde{\mathbb{Z}} \times \mathbb{R}^6 \ni (z, u) &\mapsto \tau_f(z, u) := \tau(f(z_k), f^{(1)}(z_k, z_d), f^{(2)}(z, u)) \in \mathbb{R}^3, \end{aligned} \quad (18)$$

where n_f is the unit vector associated to the function f , ω_f is the angular velocity of n_f , and finally τ_f is the angular acceleration of n_f . It follows from the definition of τ in (16), and (14)–(15) that the angular acceleration (18) can be rewritten as

$$\tau_f(z, u) = A_{n_f}(z) + B_{n_f}(z_z)u, \quad (19)$$

with $A_{n_f}(z) \in \mathbb{R}^3$ and $B_{n_f}(z_z) \in \mathbb{R}^{3 \times 6}$ defined as

$$\begin{aligned} B_{n_f}(z) &:= \mathcal{S}(n_f(z_k)) \frac{B_f(z_k)}{\|f(z_k)\|}, \\ A_{n_f}(z) &:= \mathcal{S}(n_f(z_k)) \left(\frac{A_f(z)}{\|f(z_k)\|} - \frac{n_f(z_k)^T f^{(1)}(z_k, z_d)}{\|f(z_k)\|} \frac{f^{(1)}(z_k, z_d)}{\|f(z_k)\|} \right). \end{aligned}$$

C. Input Transformation

Let us now provide the input transformation \bar{u} illustrated in Fig. 2. For that purpose we introduce a function

$$R : \tilde{\mathbb{Z}} \times \mathbb{R}^6 \ni (z, u) \mapsto R(z, u) \in \mathbb{R}^m \quad (20)$$

of $m \in \mathbb{N}$ *physical quantities* we wish to regulate/control, where $\tilde{\mathbb{Z}}$ is a subset of \mathbb{Z} (where the controller is defined). In particular, we wish to control 6 quantities:

- the force (or linear acceleration) along the direction of N represented in Fig. 1 (2 quantities: note that N in Fig. 1 spans a two dimensional space – provided that n_1 and n_2 are not co-linear – and thus we can only control two forces);
- the angular acceleration of the unit vector associated to N (2 quantities: the angular acceleration is three dimensional, but orthogonal to N ; thus we can only control two components of that torque);
- the angular acceleration of the angle between the cables (1 quantity, which we will name $\tau_\theta \in \mathbb{R}$);
- and finally the angular acceleration on the yaw position (1 quantity, which we will name $\tau_\psi \in \mathbb{R}$).

With the above in mind, let us define

$$\begin{aligned} \mathbb{Z}_{k,N} &:= \{z_k \in \mathbb{Z}_k : n_1(z_k)^T n_2(z_k) \neq -1\}, \\ N : \mathbb{Z}_{k,N} \ni z_k &\mapsto N(z_k) := w_1 n_1(z_k) + w_2 n_2(z_k) \in \mathbb{R}^3 \setminus \{0_3\}, \end{aligned} \quad (21)$$

as the vector N represented in Fig 1, for some positive convex weights w_1 and w_2 ($w_1 + w_2 = 1$; see Remark 3). We introduced in Section IV-B, how to compute the unit vector associated to N and its angular velocity and acceleration, namely n_N , ω_N and τ_N (see (17)–(18) and (19)). Define also

$$\mathbb{Z}_{k,\theta} := \{z_k \in \mathbb{Z}_k : n_1(z_k)^T n_2(z_k) \neq \pm 1\}, \quad (22)$$

$$\theta : \mathbb{Z}_{k,\theta} \ni z_k \mapsto \theta(z_k) := \arccos(n_1(z_k)^T n_2(z_k)) \in (0, \pi), \quad (23)$$

as the angle between the cables, represented in Fig 1. We introduced in Section IV-B how to compute the velocity and acceleration of θ , namely $\dot{\theta}^{(1)}$ and $\dot{\theta}^{(2)}$. Finally define (below, denote $\delta(z_k) \equiv \Pi(e_3)(n_1(z_k) - n_2(z_k))$, $c \equiv \frac{e_3^T \delta(z_k)}{\|\delta(z_k)\|}$ and

$$s \equiv \frac{e_2^T \delta(z_k)}{\|\delta(z_k)\|}$$

$$\begin{aligned} \mathbb{Z}_{k,\psi} &:= \{z_k \in \mathbb{Z}_k : \|\delta(z_k)\| > 0\}, \\ \psi : \mathbb{Z}_{k,\psi} \ni z_k &\mapsto \psi(z_k) := \frac{1}{2} \arctan(c^2 - s^2, 2cs) \in \left(-\frac{\pi}{2}, \frac{\pi}{2}\right] \simeq_{\text{isomorphic}} \mathbb{R} \setminus \sim, \\ \mathbb{R} \setminus \sim &:= \{[\psi] \subset \mathbb{R} : [\psi] := \{\dots, \psi - \pi, \psi, \psi + \pi, \dots\}\}, \end{aligned} \quad (24)$$

as the yaw position of the plane formed by the cables. We introduced in Section IV-B how to compute the velocity and acceleration of ψ , namely $\psi^{(1)}$ and $\psi^{(2)}$. For convenience, define (which will become clear next),

$$\mathbb{Z}_{k,\text{inv}} := \{z_k \in \mathbb{Z}_k : e_3^T n_{i \in \{1,2\}}(z_k) > 0, n_1(z_k)^T n_2(z_k) > 0\}, \quad (25)$$

With the above in mind, define the function R in (20), with

$$\tilde{\mathbb{Z}}_k := \mathbb{Z}_{k,N} \cap \mathbb{Z}_{k,\theta} \cap \mathbb{Z}_{k,\psi} \cap \mathbb{Z}_{k,\text{inv}}, \quad (26)$$

$$\tilde{\mathbb{Z}} := \{z := (z_k, z_d) \in \mathbb{Z} : z_k \in \tilde{\mathbb{Z}}_k\}, \quad (27)$$

and as

$$R(z, u) := \begin{bmatrix} \frac{1}{m} \sum_{i \in \{1,2\}} T_i(z, u) n_i(z_k) \\ \tau_N(z, u) \\ \theta^{(2)}(z, u) \\ \psi^{(2)}(z, u) \end{bmatrix} \stackrel{(9)}{=} \underbrace{\begin{bmatrix} \frac{1}{m} \sum_{i \in \{1,2\}} T_i(z, 0_6) \\ A_{n_N}(z) \\ A_\theta(z) \\ A_\psi(z) \end{bmatrix}}_{=: A_R(z) \in \mathbb{R}^6} + \underbrace{\begin{bmatrix} \frac{1}{m} \sum n_i(z_k) e_1^T M_T(z_k) \\ B_{n_N}(z_k) \\ B_\theta(z_k) \\ B_\psi(z_k) \end{bmatrix}}_{=: B_R(z_k) \in \mathbb{R}^{6 \times 6}} \begin{bmatrix} u_1 \\ u_2 \end{bmatrix}. \quad (28)$$

Denote $\nu = (T, \tau_N, \tau_\theta, \tau_\psi) \in \mathbb{R}^{1+3+1+1}$, and given any $z \in \tilde{\mathbb{Z}}$ define

$$\bar{\nu}(z, \nu) := (T n_N(z_k), \Pi(n_N(z_k)) \tau_N, \tau_\theta, \tau_\psi). \quad (29)$$

We note that there exists a unique $\bar{u} : \tilde{\mathbb{Z}} \times \mathbb{R}^6 \ni (z, \nu) \mapsto \bar{u}(z, \nu) \in \mathbb{R}^6$ such that $\bar{\nu}(z, \nu) = R(z, \bar{u}(z, \nu))$ and it is given by

$$\bar{u}(z, \nu) := (B_R(z_k)^T B_R(z_k))^{-1} B_R(z_k)^T (\bar{\nu}(z, \nu) - A_R(z)). \quad (30)$$

Notice that there exists an inverse on (30), which depends exclusively on the kinematic configuration, and it can be shown that (30) is well defined for any $z_k \in \tilde{\mathbb{Z}}_k$ with $\tilde{\mathbb{Z}}_k$ as in (27): $\mathbb{Z}_{k,N} \cap \mathbb{Z}_{k,\theta} \cap \mathbb{Z}_{k,\psi}$ is necessary as the domain where N , θ and ψ are defined, while $\mathbb{Z}_{k,\text{inv}}$ is necessary for invertibility. That the inverse exists can be easily shown (though after lengthy computations), once one realizes that there is a cascaded structure: first one can control the tensions as they depend exclusively on $n_1^T u_1$ and $n_2^T u_2$ (see (9)). Secondly, one may control the angular acceleration of n_N as it depends loosely speaking on $\Pi(n_N(z)) (u_1 + u_2)$. Thirdly, one may control the angular acceleration of θ and ψ , which depend loosely speaking on $\Pi(n_N(z)) (u_1 - u_2)$: controlling the angular acceleration of θ requires the first condition in (25) to be satisfied, while controlling the angular acceleration of ψ requires the second condition in (25) to be satisfied.

Indeed (and with the aforementioned in mind), the input transformation \bar{u} in (30) can be equivalently written as

$$\begin{aligned} \bar{u}_1(z, \nu) &:= \bar{u}_3(z, (T, \tau, \tau_\theta, \bar{\tau}_\psi)) \Big|_{\bar{\tau}_\psi = \frac{\delta(z_k)^T \delta(z_k) \sqrt{1 - (n_1(z_k)^T n_2(z_k))^2}}{\left(\frac{1}{w_1} + \frac{1}{w_2}\right) (e_1^T n_1(z_k) + e_1^T n_2(z_k) (n_1(z_k)^T n_2(z_k) - 1))} (\tau_\psi - (A_\psi(z) + B_\psi(z_k) \bar{u}_3(T, \tau, 0, 0)))}, \text{ where} \\ \bar{u}_3(z, \nu) &:= \bar{u}_2(z, (T, \tau, \bar{\tau}_\theta, \tau_\psi)) \Big|_{\bar{\tau}_\theta = \frac{w_1 w_2 (w_1 + w_2 n_1(z_k)^T n_2(z_k)) (w_2 + w_1 n_1(z_k)^T n_2(z_k))}{\sqrt{N(z_k)^T N(z_k)}} (\tau_\theta - (A_\theta(z) + B_\theta(z_k) \bar{u}_2(T, \tau, 0, 0)))}, \text{ where} \\ \bar{u}_2(z, \nu) &:= \bar{u}_1(z, T) + \dots, \text{ where} \\ &\left[\begin{array}{l} \frac{l_1 m_1}{w_1} \left\{ \left(\frac{\tau_\theta}{n_1(z_k)^T n_N(z_k)} + \frac{N(z_k)^T N(z_k)}{(w_1 + w_2)(1 + n_1(z_k)^T n_2(z_k))} \bar{\tau}^T \frac{\mathcal{S}(n_N(z_k)) n_1(z_k)}{\|S(n_N(z_k)) n_1(z_k)\|} \right) \frac{\Pi(n_1(z_k)) n_N(z_k)}{\|\Pi(n_1(z_k)) n_N(z_k)\|} + \dots \right. \\ \quad \left. \dots + \left(\tau_\psi + \frac{\sqrt{N(z_k)^T N(z_k)}}{2} \bar{\tau}^T \frac{\Pi(n_N(z_k)) n_1(z_k)}{\|\Pi(n_N(z_k)) n_1(z_k)\|} \right) \frac{\mathcal{S}(n_1(z_k)) n_N(z_k)}{\|S(n_1(z_k)) n_N(z_k)\|} \right\} \\ \frac{l_2 m_2}{w_2} \left\{ \left(\frac{\tau_\theta}{n_2(z_k)^T n_N(z_k)} + \frac{N(z_k)^T N(z_k)}{(w_1 + w_2)(1 + n_1(z_k)^T n_2(z_k))} \bar{\tau}^T \frac{\mathcal{S}(n_N(z_k)) n_2(z_k)}{\|S(n_N(z_k)) n_2(z_k)\|} \right) \frac{\Pi(n_2(z_k)) n_N(z_k)}{\|\Pi(n_2(z_k)) n_N(z_k)\|} + \dots \right. \\ \quad \left. \dots + \left(\tau_\psi + \frac{\sqrt{N(z_k)^T N(z_k)}}{2} \bar{\tau}^T \frac{\Pi(n_N(z_k)) n_2(z_k)}{\|\Pi(n_N(z_k)) n_2(z_k)\|} \right) \frac{\mathcal{S}(n_2(z_k)) n_N(z_k)}{\|S(n_2(z_k)) n_N(z_k)\|} \right\} \end{array} \right] \Big|_{\bar{\tau} = \tau - (A_{n_N}(z) + B_{n_N}(z_k) \bar{u}_2(T, \tau, 0, 0))} \\ \bar{u}_1(z, T) &:= \begin{bmatrix} \bar{u}_1 n_1(z_k) \\ \bar{u}_2 n_2(z_k) \end{bmatrix} \Big|_{\begin{bmatrix} \bar{u}_1 \\ \bar{u}_2 \end{bmatrix} = \begin{bmatrix} \frac{m_1}{m} & 0 \\ 0 & \frac{m_1}{m} \end{bmatrix} M_T(z_k) \left(\frac{m T}{\sqrt{N(z_k)^T N(z_k)}} \begin{bmatrix} w_1 \\ w_2 \end{bmatrix} - T(z, 0_6) \right)}. \end{aligned}$$

The mapping \bar{u} provides the input transformation shown in Fig. 2.

Remark 2: From Fig. 1, the linear acceleration of the load along the direction N is given by $n_N(z_k)^T \sum_{i \in \{1,2\}} \frac{T_i}{m} n_i(z_k)$, and with the choice made in (30) – see the first two components in (28) – the latter simplifies as T which means \ddot{T} in (29) represents the linear acceleration of the load along the green direction in Fig. 1 and which is an input we design later.

Remark 3: Consider Problem 1 with $\mathbb{R} \ni t \mapsto p^*(t) = \bar{p} \in \mathbb{R}^3$, i.e., suppose we wish the load to be at a constant position, namely \bar{p} . One can compute the equilibria $\bar{z} \in \mathbb{Z}$ and equilibria input $\bar{u} \in \mathbb{R}^6$, for which $Z(\bar{z}, \bar{u}) = 0_{18}$, and it holds that for almost all equilibria $\frac{T_1(\bar{z}, \bar{u})}{T_2(\bar{z}, \bar{u})} = \frac{w_1}{w_2}$. Thus, the ratio $\frac{w_1}{w_2}$ may be chosen so as to distribute the weight of the load onto each UAV in a desirable way.

D. State Transformation

Let us now provide the coordinate transformation illustrated in Fig. 2, which will expose the three decoupled problems illustrated in that figure. Define then the state sets

$$\mathbb{X}_1 := \{x_1 := (p, v, n, \omega) \in (\mathbb{R}^3)^4 : n \in \mathbb{S}^2, \omega^T n = 0\}, \quad (31a)$$

$$\mathbb{X}_2 := \{x_2 := (\theta, \omega_\theta) \in \mathbb{R}^2 : \theta \in (0, \pi)\}, \quad (31b)$$

$$\mathbb{X}_3 := \{x_3 := (\psi, \omega_\psi) \in \mathbb{R}^2\}. \quad (31c)$$

We always decompose an $x_1 \in \mathbb{X}_1$, an $x_2 \in \mathbb{X}_2$ and an $x_3 \in \mathbb{X}_3$ as decomposed in (31a)–(31c). Consider then the mapping

$$\mathbb{Z} \ni z \mapsto g(z) := (g_1(z), g_2(z), g_3(z)) \in \mathbb{X}_1 \times \mathbb{X}_2 \times \mathbb{X}_3 \quad (32)$$

where

$$\mathbb{Z} \ni z \mapsto g_1(z) := \begin{bmatrix} p \\ v \\ n_N(z_k) \\ \omega_N(z_k, z_d) \end{bmatrix} \in \mathbb{X}_1, \quad (33a)$$

$$\mathbb{Z} \ni z \mapsto g_2(z) := \begin{bmatrix} \theta(z_k) \\ \theta^{(1)}(z_k, z_d) \end{bmatrix} \in \mathbb{X}_2, \quad (33b)$$

$$\mathbb{Z} \ni z \mapsto g_3(z) := \begin{bmatrix} \psi(z_k) \\ \psi^{(1)}(z_k, z_d) \end{bmatrix} \in \mathbb{X}_3, \quad (33c)$$

where g_1 in (33a) isolates the position of the load, the velocity of the load, the unit vector given by N (see Fig. 1) and its angular velocity. g_2 in (33b) isolates the angle between the cables, and its angular velocity; and g_3 in (33c) isolates the yaw position and its angular velocity (all the functions in (33a)–(33c) are those introduced in Sections IV-C and IV-B). The mapping g in (32) is invertible – its inverse is found in the mathematica file, but we can proceed without having to compute its inverse.

It follows after simple calculations that (denote $\nu_1 := (T, \tau) \in \mathbb{R}^{1+3}$)

$$Dg_1(z)Z(z, \bar{u}(z, \nu)) = \begin{bmatrix} v \\ Tn_N(z_k) - ge_3 \\ \mathcal{S}(\omega_N(z_k, z_d))n_N(z_k) \\ \Pi(n_N(z_k))\tau \end{bmatrix} \left(= \begin{bmatrix} \dot{p} \\ \dot{v} \\ \dot{n}_N \\ \dot{\omega}_N \end{bmatrix} = \dot{x}_1 \right) \quad (34)$$

$$Dg_2(z)Z(z, \bar{u}(z, \nu)) = \begin{bmatrix} \theta^{(1)}(z_k, z_d) \\ \tau_\theta \end{bmatrix} \left(= \begin{bmatrix} \dot{\theta} \\ \dot{\omega}_\theta \end{bmatrix} = \dot{x}_2 \right), \quad (35)$$

$$Dg_3(z)Z(z, \bar{u}(z, \nu)) = \begin{bmatrix} \psi^{(1)}(z_k, z_d) \\ \tau_\psi \end{bmatrix} \left(= \begin{bmatrix} \dot{\psi} \\ \dot{\omega}_\psi \end{bmatrix} = \dot{x}_3 \right). \quad (36)$$

The choice of the control input (30) and the mappings (33a)–(33c) is now clear: it induces three decoupled vector fields, namely those in (34), (35) and (36). The vector fields (35) and (36) are those of double integrators, while the vector field in (34) is that of a thrust propelled system. Since these vector fields are decoupled, we can design control laws for $\nu_1 \equiv (T, \tau)$, $\nu_2 \equiv \tau_\theta$ and $\nu_3 \equiv \tau_\psi$ separately.

V. SEPARATE CONTROL LAWS

We must now develop three control laws for the three decoupled systems, as illustrated in Fig. 2. Recall however that the mapping \bar{u} , in (30) and illustrated in Fig. 2, which allows for the decoupling is only well defined for a subset of the kinematic space. Indeed, it is well defined for all $z \in \tilde{\mathbb{Z}} \Leftrightarrow z_k \in \tilde{\mathbb{Z}}_k$ (see (26) and (27)). As such, the control design idea that we follow next is to assume that $z_k(0) \in \tilde{\mathbb{Z}}_k$, and to develop controllers which guarantee that $z_k(t) \in \tilde{\mathbb{Z}}_k$ for all $t \geq 0$, thus guaranteeing well-posedness of the control law.

A. Control of angle between the cables

We start with the control design for the angle between the cables, which we want to converge to some $\theta^* \in (0, \frac{\pi}{4})$. Recall then the vector field (35), which can be written as $\mathbb{X}_2 \ni x_2 \mapsto X_2(x_2, \tau_\theta) = (\omega_\theta, \tau_\theta) \in \mathbb{R}^2$, and that our goal is to guarantee that z_k remains in $\tilde{\mathbb{Z}}_k$ in (26). The set $\mathbb{Z}_{k,\theta}$ in (22) motivates the definition of

$$\tilde{\mathbb{X}}_2 := \left\{ (\theta, \omega_\theta) \in \mathbb{X}_2 : \theta \in \left(0, \frac{\pi}{4}\right) \right\}. \quad (37)$$

The lower bound 0 in (37) is needed because the mapping \bar{u} is not well defined when the cables overlap; the upper bound $\frac{\pi}{4}$ can only be understood in Section V-B, and it guarantees that the first two conditions in (25) are satisfied. Consider the following control law $\tilde{\mathbb{X}}_2 \ni x_2 \mapsto \tau_\theta^{cl}(x_2) \in \mathbb{R}$ defined as

$$\nu_2^{cl}(x_2) \equiv \tau_\theta^{cl}(x_2) := -k_\theta \frac{\theta - \theta^*}{\theta \left(\theta - \frac{\pi}{4}\right)} - k_{\omega_\theta} \omega_\theta \quad (38)$$

which induces the closed loop vector field $\tilde{\mathbb{X}}_2 \ni x_2 \mapsto X_2^{cl}(x_2) := X_2(x_2, \tau_\theta^{cl}(x_2))$. We emphasize that $\tau_\theta^{cl}((\theta^*, 0)) = 0$, that $\lim_{\theta \rightarrow 0} \tau_\theta^{cl}((\theta, \cdot)) = \infty$ and that $\lim_{\theta \rightarrow \pi/4} \tau_\theta^{cl}((\theta, \cdot)) = -\infty$. Moreover, it follows that for the (Lyapunov) function $\tilde{\mathbb{X}}_2 \ni x_2 \mapsto V_2(x_2) \geq 0$ defined as

$$V_2(x_2) := k_\theta \int_{s=\theta^*}^{s=\theta} \frac{s - \theta^*}{s \left(s - \frac{\pi}{4}\right)} ds + \frac{1}{2} \omega_\theta^2$$

it holds that

$$\tilde{\mathbb{X}}_2 \ni x_2 \mapsto W_2(x_2) := DV_2(x_2) X_2^{cl}(x_2) = -k_{\omega_\theta} \omega_\theta^2 \leq 0.$$

It follows from V_2 and W_2 that a solution $t \mapsto x_2(t)$ of $\dot{x}_2(t) = X_2^{cl}(x_2(t))$ with $x_2(0) \in \tilde{\mathbb{X}}_2$ never gets arbitrarily close to the boundaries of $\tilde{\mathbb{X}}_2$ (i.e., θ never gets arbitrarily close to 0 or $\frac{\pi}{4}$); and that $\lim_{t \rightarrow \infty} x_2(t) = (\theta^*, 0)$. For the quadrotors-load system this is equivalent to saying that the angle between the cables converges to a desired angle $\theta^* \in (0, \frac{\pi}{4})$; and that it never gets arbitrarily close to 0 (and thus that the UAVs collide) or arbitrarily close to $\frac{\pi}{4}$, and thus that $0 < \theta(z_k) := \arccos(n_1(z_k)^T n_2(z_k)) < \frac{\pi}{4}$ which implies that (this implication can be easily understood from Fig. 1)

$$0 < \arccos(n_i(z_k)^T n_N(z_k)) < \pi/4, \quad (39)$$

which means that z_k remains in the sets $\mathbb{Z}_{k,N}$ and $\mathbb{Z}_{k,\theta}$ in (21) and (22).

B. Control of the thrust propelled system

Recall then the vector field (34), which can be rewritten as

$$X_1 : \mathbb{R}_{\geq 0} \times \mathbb{X}_1 \times \mathbb{R}^4 \ni (t, x_1, (T, \tau)) \mapsto X_1(t, x_1, (T, \tau)) \in T_{x_1} \mathbb{X}_1$$

$$X_1(t, x_1, (T, \tau)) := \begin{bmatrix} v \\ Tn - g(t) \\ \mathcal{S}(\omega) n \\ \Pi(n) \tau \end{bmatrix} \Big|_{g(t) := g e_3 + p^{*(2)}(t)} \left(= \begin{bmatrix} \frac{d}{dt}(p - p^{*(0)}) = \frac{d}{dt}(\text{position error}) \\ \frac{d}{dt}(v - p^{*(1)}) = \frac{d}{dt}(\text{velocity error}) \\ \dot{n}_N \\ \dot{\omega}_N \end{bmatrix} \right). \quad (40)$$

Our goal is to guarantee that z_k remains in $\tilde{\mathbb{Z}}_k$ in (26), which motivates the definition

$$\tilde{\mathbb{X}}_1 := \left\{ (p, v, n, \omega) \in \mathbb{X}_1 : n^T e_3 > \frac{\pi}{4} \right\}. \quad (41)$$

The vector field in (40) is that of a thrust propelled vector field, for which controllers

$$\mathbb{R}_{\geq 0} \times \mathbb{X}_1 \ni (t, x_1) \mapsto \nu_1^{cl}(t, x_1) \equiv (T^{cl}(t, x_1), \tau^{cl}(t, x_1)) \in \mathbb{R}^4 \quad (42)$$

are found in the literature, which guarantee that $\lim_{t \rightarrow \infty} p(t) = 0_3$. In the case of (34) that corresponds to steering the position tracking error to 0_3 , and therefore to steering the position to the desired position trajectory. Suppose moreover that the controller in (42) guarantees that the set $\tilde{\mathbb{X}}_1$ is positively invariant (this is possible with the controller found in [26]). Then, it follows from the triangular inequality that

$$\begin{aligned} n_i(z_k)^T e_3 &\geq \cos(\arccos(n_i(z_k)^T n(z_k)) + \arccos(n(z_k)^T e_3)) \\ &\stackrel{(41)}{\geq} \cos\left(\arccos(n_i(z_k)^T n(z_k)) + \frac{\pi}{4}\right) \stackrel{(39)}{\geq} \cos\left(\frac{\pi}{4} + \frac{\pi}{4}\right) > 0, \end{aligned}$$

which means that z_k satisfies the first two conditions in $\mathbb{Z}_{k,\text{inv}}$ in (25).

C. Control of yaw position

Consider now the vector field (36), which can be written as $\mathbb{X}_3 \ni x_3 \mapsto X_3(x_3, \tau_\psi) := (\omega_\psi, \tau_\psi) \in \mathbb{R}^2$, and recall that our goal is to guarantee that z_k remains in $\tilde{\mathbb{Z}}_k$ in (26). Recall also (24), which motivates the definition

$$\psi_1 \sim \psi_2 : \Leftrightarrow \psi_1 - \psi_2 = k\pi, k \in \{\dots, -1, 0, 1, \dots\}, \quad (43)$$

where \sim is an equivalence relation, namely (i.e., two angles are equivalent if they differ by a multiple of half of a full rotation). Denote $\tilde{\mathbb{X}}_3 := \mathbb{X}_3$, and consider then the control law $\tilde{\mathbb{X}}_3 \ni x_3 \mapsto \tau_\psi^{cl}(x_3) \in \mathbb{R}$ defined as

$$\nu_3^{cl}(x_3) \equiv \tau_\psi^{cl}(x_3) := -k_\psi \sin(2\psi) - k_{\omega_\psi} \omega_\psi, \quad (44)$$

which induces the closed loop vector field $\tilde{\mathbb{X}}_3 \ni x_3 \mapsto X_3^{cl}(x_3) := X_3(x_3, \tau_\psi^{cl}(x_3))$; and where we emphasize that $\tau_\psi^{cl}(0_2) = 0$ and that $\lim_{\psi \rightarrow \pm\pi/2} \tau_\psi^{cl}((\psi, \cdot)) = \mp\infty$ (we also note that the control law is continuous and periodic in $(\mathbb{R} \setminus \sim) \times \mathbb{R} \simeq (-\frac{\pi}{2}, \frac{\pi}{2}] \times \mathbb{R}$). It follows that for the (Lyapunov) function $\tilde{\mathbb{X}}_3 \ni x_3 \mapsto V_3(x_3) \geq 0$ defined as

$$V_3(x_3) := k_\psi(1 - \cos(2\psi)) + \omega_\psi^2$$

it holds that

$$\tilde{\mathbb{X}}_3 \ni x_3 \mapsto W_3(x_3) := DV_3(x_3)X_3^{cl}(x_3) = -2k_{\omega_\psi}\omega_\psi^2 \leq 0.$$

It follows from V_3 and W_3 that a solution $t \mapsto x_3(t)$ of $\dot{x}_3(t) = X_3^{cl}(x_3(t))$ converges to either the equivalence class $[0] = \{k\pi : k \text{ integer}\}$ (stable) or to the equivalence class $[\frac{\pi}{2}] = \{k\frac{\pi}{2} : k \text{ integer}\}$ (unstable). We emphasize that, with the choice of ψ (in (24)) that we made, the yaw control does not see a difference between the vehicles: i.e., if, for example, when seen from a top view, vehicle 1 points North w.r.t. vehicle 2, then that corresponds to the same yaw as if vehicle 2 points North w.r.t. vehicle 1. As such, the yaw control here performed is that of the *plane* containing the vertical direction, and the two vehicles when projected onto an horizontal plane (note that, indeed, the yaw of a *plane* does not see a difference in half rotations, justifying the introduced equivalence relation).

D. Complete control law

We are now in position of providing (11), and thus (12). Consider then the control laws (38), (42) and (44), and the corresponding sets (37), (41) and (43). The set $\tilde{\mathbb{X}} := \tilde{\mathbb{X}}_1 \times \tilde{\mathbb{X}}_2 \times \tilde{\mathbb{X}}_3$ provides then the domain of the control law ν^{cl} in (11), and we note that $\{z \in \mathbb{Z} : g(z) \in \tilde{\mathbb{X}}\} \subset \tilde{\mathbb{Z}}$. The control law u^{cl} in (12) can then be implemented yielding the closed loop vector field (13). Finally, we note that an inverse of g (in (32)) exists when restricted to $\tilde{\mathbb{X}}$, i.e., there exists a g^{-1} such that

$$\begin{aligned} g^{-1}(g(z)) &= z \text{ for all } z \in \{z \in \mathbb{Z} : g(z) \in \tilde{\mathbb{X}}\} \subset \tilde{\mathbb{Z}} \text{ and,} \\ g(g^{-1}(x)) &= x \text{ for all } x \in \tilde{\mathbb{X}}. \end{aligned}$$

Theorem 4: Consider the system with vector field (6), and the control law (12), which yields the closed loop vector field (13). It follows that for any initial condition $z(0) \in \{z \in \mathbb{Z} : g(z) \in \tilde{\mathbb{X}}\} \subset \tilde{\mathbb{Z}}$, a solution of $t \mapsto z(t)$ of $\dot{z}(t) = Z^{cl}(t, z(t))$ is such that $z(t) \in \tilde{\mathbb{Z}}$ for all $t \geq 0$, $\lim_{t \rightarrow \infty} (p(t) - p^*(t)) = 0_3$, $\lim_{t \rightarrow \infty} \theta(z_k(t)) = \theta^*$ and $\lim_{t \rightarrow \infty} \psi(z_k(t)) = 0$ (with the functions θ and ψ in (23) and (24)).

Proof: Given the solution $t \mapsto z(t)$, one may compute $t \mapsto x(t) := (x_1(t), x_2(t), x_3(t)) := g(z(t))$ via the mapping g in (32). Since $z(0) \in \{z \in \mathbb{Z} : g(z) \in \tilde{\mathbb{X}}\} \subset \tilde{\mathbb{Z}}$, it follows that $x(0) := g(z(0)) \in \tilde{\mathbb{X}} := \tilde{\mathbb{X}}_1 \times \tilde{\mathbb{X}}_2 \times \tilde{\mathbb{X}}_3$. As shown in Sections V-A–V-C, the control laws guarantee that $t \mapsto x(t)$ does not get arbitrarily close to the boundaries of $\tilde{\mathbb{X}}$, and thus, $t \mapsto z(t) = g^{-1}(x(t))$ does also not get arbitrarily close to the boundaries of $\tilde{\mathbb{Z}}$. This guarantees then that the control law (12) is always well defined. Moreover, it was also concluded in the same sections, that $\lim_{t \rightarrow \infty} p(t) - p^*(t) = 0_3$ ($x_1 = (p, v, n, \omega)$), that $\lim_{t \rightarrow \infty} \theta(t) = \theta^*$ ($x_2 = (\theta, \omega)$) and that $\lim_{t \rightarrow \infty} \psi(t) \in [0]$ or $[\frac{\pi}{2}]$ ($x_3 = (\psi, \omega)$; equivalence class $[\frac{\pi}{2}]$ is unstable), justifying the theorem's conclusions. ■

VI. ATTITUDE CONTROL

In Section III, we assumed that the quadrotors were fully actuated, which is not the case in a real aerial vehicle. Consider then the augmented state

$$\begin{aligned} \bar{z} &= (z, r_1, r_2) \in \mathbb{Z} \times \mathbb{S}^2 \times \mathbb{S}^2 =: \bar{\mathbb{Z}}, \\ x_4 &= ((x_1, x_2, x_3), r_1, r_2) \in (\mathbb{X}_1 \times \mathbb{X}_2 \times \mathbb{X}_3) \times \mathbb{S}^2 \times \mathbb{S}^2 =: \mathbb{X}_4, \end{aligned}$$

where $r_1, r_2 \in \mathbb{S}^2$ stand for the quadrotors' direction where input thrust is provided (see Fig. 1); and with z as in (2) and x_1, x_2, x_3 as in (31a), (31b), (31c). The state $\bar{z} : \mathbb{R}_{\geq 0} \ni t \mapsto \bar{z}(t) \in \bar{\mathbb{Z}}$ evolves according to $\dot{\bar{z}}(t) = \bar{Z}(\bar{z}(t), u(t))$, $\bar{z}(0) \in \bar{\mathbb{Z}}$,

where $\bar{Z} : \bar{\mathbb{Z}} \times \mathbb{R}^8 \ni (\bar{z}, u) \mapsto \bar{Z}(\bar{z}, u) \in T_{\bar{z}}\bar{\mathbb{Z}}$ is given by (denote $u := (U_1, U_2, \omega_{r_2}, \omega_{r_1}) \in \mathbb{R}^{2+6}$)

$$\bar{Z}(\bar{z}, u) := \begin{bmatrix} Z(z, (U_1 r_1, U_2 r_2)) \\ \mathcal{S}(\omega_{r_1}) r_1 \\ \mathcal{S}(\omega_{r_2}) r_2 \end{bmatrix} \begin{pmatrix} \dot{z} \\ \dot{r}_1 \\ \dot{r}_2 \end{pmatrix}, \quad (45)$$

with the vector field Z as in (6). One must now design control laws for the thrusts (U_1 and U_2) and angular velocities (ω_{r_1} and ω_{r_2}) for each quadrotor. Given the control law (12), one may be tempted to choose $\mathbb{R}_{\geq 0} \times \bar{\mathbb{Z}} \ni (t, \bar{z}) \mapsto U_i^{cl}(t, \bar{z}) := r_i^T u_i^{cl}(t, z) \in \mathbb{R}$, as it minimizes the error to the desired input, i.e., $U_i^{cl}(t, \bar{z}) = \inf_{U_i \in \mathbb{R}} \|U_i r_i - u_i^{cl}(t, z)\|$. However, if that choice is made, the vector field (34) would be corrupted by an error of the type $(0_3, \star_3, 0_3, \star_3)$. This however invalidates the use of most hierarchical control laws (42) in the literature, which rely on the cascaded structure of (34) [25], [26]. We solve this problem next. Notice that given any $u \in \mathbb{R}^3$ and $n, r \in \mathbb{S}^2$ with $n^T r \neq 0$, the equality $\frac{n^T u}{n^T r} r = u + \frac{1}{n^T r} \mathcal{S}(n) \mathcal{S}(r) u$ holds. With that in mind, let $\tilde{\mathbb{Z}} := \{\bar{z} \in \bar{\mathbb{Z}} : z \in \tilde{\mathbb{Z}}, r_i^T n_i(z_k) > 0, i \in \{1, 2\}\}$ and consider the throttle control law $\mathbb{R}_{\geq 0} \times \tilde{\mathbb{Z}} \ni (t, \bar{z}) \mapsto U_i^{cl}(t, \bar{z}) \in \mathbb{R}$ defined as

$$U_i^{cl}(t, \bar{z}) := \frac{n_i(z_k)^T u_i^{cl}(t, z)}{n_i(z_k)^T r_i} =: u_i^{cl}(t, z) + e_{4,i}(t, \bar{z}), \quad (46)$$

where the error

$$e_{4,i}(t, \bar{z}) := \frac{\mathcal{S}(n_i(z_k)) \mathcal{S}(r_i) u_i^{cl}(t, z)}{r_i^T n_i(z_k)}$$

is orthogonal to the cable i (i.e., to n_i). Notice from (9) that the tensions depend on $n_1^T u_1$ and $n_2^T u_2$, and thus, it follows that with the choice in (46) the tensions remain unchanged; i.e., it follows from composing (28) with (46) that

$$R(z, (U_1^{cl}(t, \bar{z}) r_1, U_2^{cl}(t, \bar{z}) r_2)) = R(z, u^{cl}(t, z)) + \begin{bmatrix} 0_{3 \times 6} \\ B_{n_N}(z_k) \\ B_\theta(z_k) \\ B_\psi(z_k) \end{bmatrix} \begin{bmatrix} e_{4,1}(t, \bar{z}) \\ e_{4,2}(t, \bar{z}) \end{bmatrix}$$

Given the mapping

$$\bar{g} : \tilde{\mathbb{Z}} \ni \bar{z} \mapsto \bar{g}(\bar{z}) := (g(z), r_1, r_2)$$

it follows that

$$D\bar{g}(\bar{z})\bar{Z}(\bar{z}, (U_1^{cl}(t, \bar{z}), U_2^{cl}(t, \bar{z}), \omega_{r_1}, \omega_{r_2}))|_{\bar{z}=\bar{g}^{-1}(t, x_4)} = \begin{bmatrix} X_1(x_1, \nu_1^{cl}(t, x_1)) + e_1(t, \bar{z}) \\ X_2(x_2, \nu_2^{cl}(t, x_2)) + e_2(t, \bar{z}) \\ X_3(x_3, \nu_3^{cl}(t, x_3)) + e_3(t, \bar{z}) \\ 0_3 \\ 0_3 \end{bmatrix} + \begin{bmatrix} 0_{18} \\ \mathcal{S}(\omega_{r_1}) r_1 \\ \mathcal{S}(\omega_{r_2}) r_2 \end{bmatrix}$$

where

$$\begin{aligned} e_1(t, z) &= \begin{bmatrix} 0_{9 \times 6} \\ B_{n_N}(z_k) \end{bmatrix} \begin{bmatrix} e_{4,1}(t, \bar{z}) \\ e_{4,2}(t, \bar{z}) \end{bmatrix}, \\ e_2(t, z) &= \begin{bmatrix} 0_{1 \times 6} \\ B_\theta(z_k) \end{bmatrix} \begin{bmatrix} e_{4,1}(t, \bar{z}) \\ e_{4,2}(t, \bar{z}) \end{bmatrix}, \\ e_3(t, z) &= \begin{bmatrix} 0_{1 \times 6} \\ B_\psi(z_k) \end{bmatrix} \begin{bmatrix} e_{4,1}(t, \bar{z}) \\ e_{4,2}(t, \bar{z}) \end{bmatrix}. \end{aligned} \quad (47)$$

Because the error e_1 in (47) has the form $(0_9, \star_3)$, the hierarchical control laws (42) from the literature can be used. One can then define the desired quadrotor $i \in \{1, 2\}$ attitude

$$\mathbb{R}_{\geq 0} \times \tilde{\mathbb{Z}} \ni (t, z) \mapsto r_i^{cl}(t, z) := \frac{u_i^{cl}(t, z)}{\|u_i^{cl}(t, z)\|} \in \mathbb{S}^2,$$

compute its angular velocity $\mathbb{R}_{\geq 0} \times \tilde{\mathbb{Z}} \ni (t, \bar{z}) \mapsto \omega_{r_i}^{cl}(t, \bar{z}) \in \mathbb{R}^3$, and construct the control law $\mathbb{R}_{\geq 0} \times \tilde{\mathbb{Z}} \ni (t, \bar{z}) \mapsto \omega_i^{cl}(t, \bar{z}) \in \mathbb{R}^3$ defined as

$$\omega_i^{cl}(t, \bar{z}) := \omega_{r_i}^{cl}(t, \bar{z}) - k_{r_\theta} \mathcal{S}(r_i^{cl}(t, z)) r_i. \quad (48)$$

It follows that the Lyapunov function $\mathbb{R}_{\geq 0} \times \tilde{\mathbb{Z}} \ni (t, \bar{z}) \mapsto V(t, \bar{z}) := \sum (1 - r_i^T r_i^{cl}(t, z)) > 0$ has a non-positive derivative along the closed loop vector field, specifically $\mathbb{R}_{\geq 0} \times \tilde{\mathbb{Z}} \ni (t, \bar{z}) \mapsto W(t, \bar{z}) = -\sum_{i \in \{1, 2\}} k_{\theta r} \|\mathcal{S}(r_i) r_i^{cl}(t, z)\|^2 \leq 0$. This guarantees that $t \mapsto \mathcal{S}(r_i(t)) r_i^{cl}(t, z(t))$ converges exponentially fast to 0_3 . As such, so does $t \mapsto e_{4,1}(t, \bar{z}(t))$ and $t \mapsto e_{4,2}(t, \bar{z}(t))$ and consequently so do the errors in (47). Then, if k_{r_θ} is large enough, the result below follows, where it is

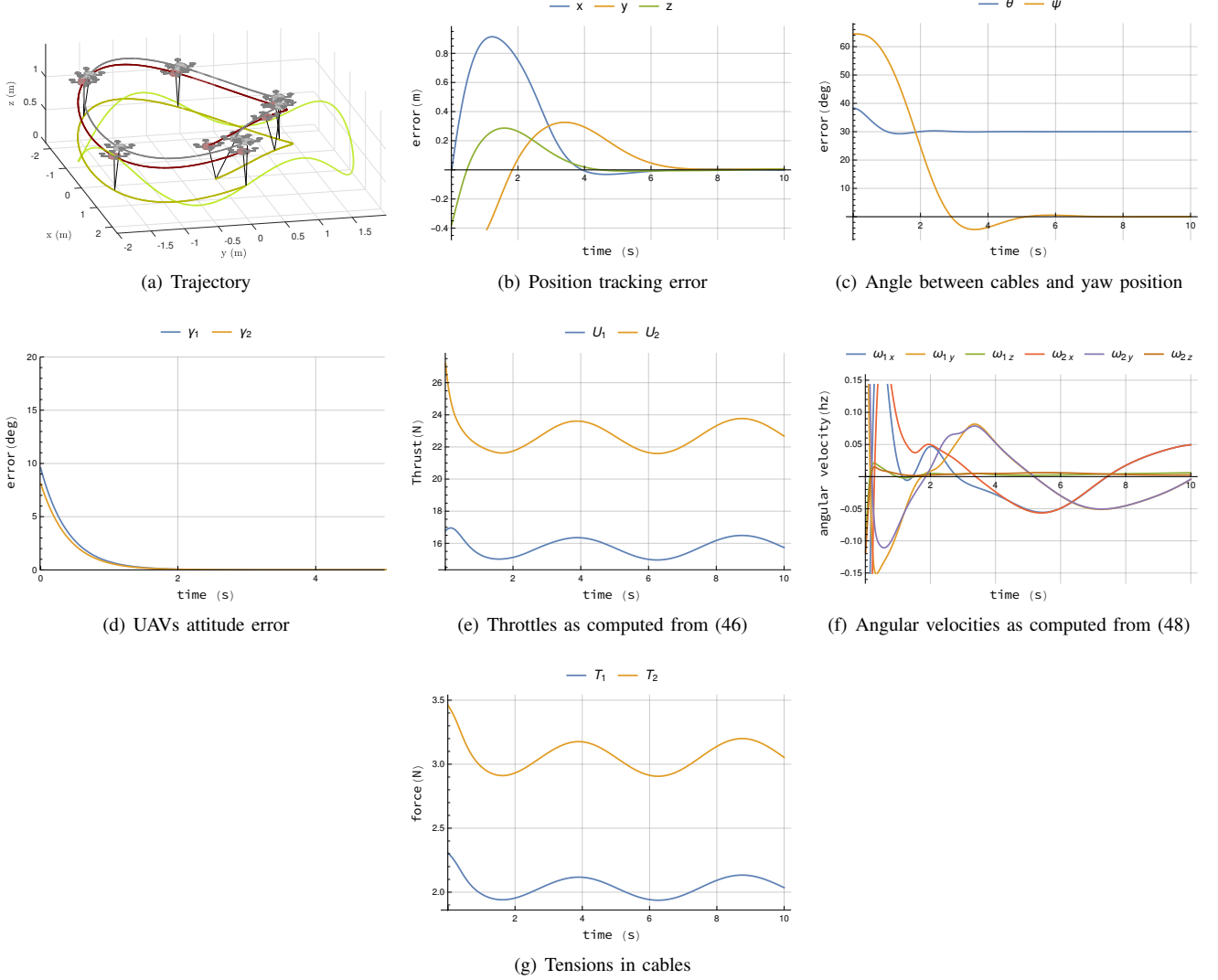


Fig. 3: Trajectory for vector field (45).

necessary to assume that $\bar{z}(t) \in \tilde{\mathbb{Z}}$ and that $\|u_i^{cl}(t, z(t))\| \neq 0$ for all $t \geq 0$, so that (46) and the desired quadrotor directions r_1^{cl}, r_2^{cl} are well defined.

Theorem 5: Given the vector field (45), the throttle control laws (46) and the angular velocity control laws (48), Theorem's 4 conclusions hold for some large enough $k_{r_\theta} > 0$, and provided that the solution $t \mapsto \bar{z}(t)$ lies in $\tilde{\mathbb{Z}}$ and that $\|u_i^{cl}(t, z(t))\| \neq 0$ for all $t \geq 0$.

Remark 6: The vector field (45) could also be extended to the case where we have control over the torques on the vehicles, rather than their angular velocities.

Remark 7: The yaw motion of the quadrotor $i \in \{1, 2\}$ can be controlled by appropriately designing the component of ω_{r_i} aligned with r_i . However, since the yaw motion of the quadrotor does not affect the motion of the load, we omit this design step in the paper. See also [25, page 71].

VII. SIMULATIONS

Consider the system quadrotors-load with parameters $m = 0.5\text{kg}$, $m_1 = 1.4\text{kg}$, $m_2 = 2.0\text{kg}$, $l_1 = 0.5\text{m}$, $l_2 = 0.7\text{m}$, $w_1 = 0.4$ and $w_2 = 0.6$. The desired position trajectory is

$$\mathbb{R}_{\geq 0} \ni t \mapsto p^*(t) := (2 \cos(\pi/5t), 2 \sin(\pi/5t), 0.5 + 0.3 \sin(\pi/2.5t))(\text{m}) \in \mathbb{R}^3,$$

and the desired angle between the cables is $\theta^* = 30^\circ$. The gains of the chosen control laws are found in the companion mathematica files (the control law (42) is that from [26]). For these choices, we provide a simulation in Fig. 3, as a solution $t \mapsto \bar{z}(t) \in \tilde{\mathbb{Z}}$ of (45) composed with the proposed control law ((46) and (48)) and with $\bar{z}(0) = (0_3, p_1, p_2, 0_3, e_3, e_3) \in \tilde{\mathbb{Z}}$,

with $p_1 \approx (0.05, 0.07, 0.49) \in \mathbb{R}^3$ and $p_2 \approx (-0.07, -0.10, 0.69) \in \mathbb{R}^3$. In Fig. 3(a), one can visualize the quadrotors-load trajectory, and a visual inspection indicates the desired position is tracked. In Figs. 3(b), the position errors are shown, and one verifies that indeed the error position ($t \mapsto p(t) - p^*(t)$) is steered to zero. In Figs. 3(c), the angle between the cables and the yaw position are shown, and one verifies that $t \mapsto \theta(z_k(t))$ converges to the desired angle $\theta^* = 30^\circ$, while $t \mapsto \psi(z_k(t))$ converges to 0. In Figs 3(e) and (3(f)), the throttle and angular velocity inputs computed from (46) and (48) are shown. In Fig. 3(d), one verifies that the quadrotors attitude converges to the desired attitude, i.e., that $t \mapsto \gamma_i(t) := \arccos(r_i(t)^T r_i^{cl}(t)) := \arccos\left(r_i(t)^T \frac{u_i^{cl}(z(t))}{\|u_i^{cl}(z(t))\|}\right)$ for $i \in \{1, 2\}$ is steered to zero. Finally, in Fig. 3(g) one can visualize the tensions in the cables $t \mapsto T_i(z(t), (U_1^{cl}(t, \bar{z}(t))r_1(t), U_1^{cl}(t, \bar{z}(t))r_2(t)))$ with U_i^{cl} as in (46) for $i \in \{1, 2\}$, and one verifies that those tensions are always positive, which means the cables are always taut. Recall from Remark 3 that, for a stationary desired trajectory, $T_1/T_2 = w_1/w_2 = 2/3$, and it can be seen in Fig. 3(g) that that is met approximately for non-stationary trajectories. Deriving precise conditions on the initial state that guarantee that the tensions remain positive has been left for future research.

VIII. CONCLUSIONS

In this paper, we modeled a point mass load tethered to two aerial vehicles, and proposed a framework for trajectory tracking of the load. Our framework consisted in designing an input and a state transformation which converted the quadrotors-load system into three decoupled subsystems. One subsystem, concerning the position of the load, has dynamics similar to those of an under-actuated aerial vehicle, allowing us to leverage control strategies that are found in the literature. Another subsystem is related to the angle between the cables, with which we can guarantee that the transporting aerial vehicles do not collide. The third subsystem is related to the yaw motion of the plane formed by the cables.

REFERENCES

- [1] AEROWORKS aim. Retrieved from <http://www.aeroworks2020.eu/>. September, 2016.
- [2] F. Kendoul. Survey of advances in guidance, navigation, and control of unmanned rotorcraft systems. *Journal of Field Robotics*, 29(2):315–378, 2012.
- [3] N. Michael, J. Fink, and V. Kumar. Cooperative manipulation and transportation with aerial robots. *Autonomous Robots*, 30(1):73–86, 2011.
- [4] M. Orsag, C. M. Korpela, S. Bogdan, and P. Y. Oh. Hybrid adaptive control for aerial manipulation. *Journal of Intelligent & Robotic Systems*, 73(1):693–707, 2013.
- [5] J.L.J. Scholten, M. Fumagalli, S. Stramigioli, and R. Carloni. Interaction control of an UAV endowed with a manipulator. In *IEEE International Conference on Robotics and Automation (ICRA)*, pages 4910–4915, May 2013.
- [6] H. Lee, H. Kim, and H.J. Kim. Path planning and control of multiple aerial manipulators for a cooperative transportation. In *IEEE/RSJ International Conference on Intelligent Robots and Systems (IROS)*, pages 2386–2391, Sept 2015.
- [7] G. Wu and K. Sreenath. Geometric control of multiple quadrotors transporting a rigid-body load. In *53rd IEEE Conference on Decision and Control*, pages 6141–6148, Dec 2014.
- [8] T. Lee. Geometric control of multiple quadrotor UAVs transporting a cable-suspended rigid body. In *Conference on Decision and Control*, pages 6155–6160. IEEE, 2014.
- [9] P. O. Pereira, R. Zanella, and D. V. Dimarogonas. Decoupled design of controllers for aerial manipulation with quadrotors. In *2016 IEEE/RSJ International Conference on Intelligent Robots and Systems (IROS)*, pages 4849–4855, Oct 2016.
- [10] M. E. Guerrero, D. A. Mercado, R. Lozano, and C. D. Garcia. Passivity based control for a quadrotor UAV transporting a cable-suspended payload with minimum swing. In *2015 54th IEEE Conference on Decision and Control (CDC)*, pages 6718–6723, Dec 2015.
- [11] T. K. Lau. An initialization method for monocular visual localization of miniature aerial robots. In *2011 50th IEEE Conference on Decision and Control and European Control Conference*, pages 3533–3538, Dec 2011.
- [12] R. Mahony, S. Stramigioli, and J. Trumpf. Vision based control of aerial robotic vehicles using the port hamiltonian framework. In *2011 50th IEEE Conference on Decision and Control and European Control Conference*, pages 3526–3532, Dec 2011.
- [13] M. Bisgaard, A. la Cour-Harbo, and J. Bendtsen. Full state estimation for helicopter slung load system. In *AIAA Guidance, Navigation and Control Conference and Exhibit*, page 6762, 2007.
- [14] P. E.I. Pounds, D.R. Bersak, and A.M. Dollar. Grasping from the air: Hovering capture and load stability. In *IEEE International Conference on Robotics and Automation (ICRA)*, pages 2491–2498, May 2011.
- [15] M. Bisgaard, J. D. Bendtsen, and A. L. Cour-Harbo. Modeling of generic slung load system. *Journal of guidance, control, and dynamics*, 32(2):573–585, 2009.
- [16] M. Bernard and K. Kondak. Generic slung load transportation system using small size helicopters. In *International Conference on Robotics and Automation*, pages 3258–3264. IEEE, 2009.
- [17] M. Bisgaard, A. Cour-Harbo, E. N. Johnson, and J. D. Bendtsen. Vision aided state estimator for helicopter slung load system. *17th IFAC Symposium on Automatic Control in Aerospace*, 2007.
- [18] I. Palunko, P. Cruz, and R. Fierro. Agile load transportation. *IEEE Robotics Automation Magazine*, 19(3):69–79, 9 2012.
- [19] K. Sreenath, N. Michael, and V. Kumar. Trajectory generation and control of a quadrotor with a cable-suspended load - A differentially-flat hybrid system. In *International Conference on Robotics and Automation*, pages 4888–4895. IEEE, 2013.
- [20] É. Servais, H. Mounier, and B. d’Andréa Novel. Trajectory tracking of trirotor UAV with pendulum load. In *20th International Conference on Methods and Models in Automation and Robotics (MMAR)*, pages 517–522, Aug 2015.
- [21] T. Lee, K. Sreenath, and V. Kumar. Geometric control of cooperating multiple quadrotor UAVs with a suspended payload. In *Conference on Decision and Control*, pages 5510–5515. IEEE, 2013.
- [22] P. Pereira, M. Herzog, and D. V. Dimarogonas. Slung load transportation with single aerial vehicle and disturbance removal. In *Mediterranean Conference on Control and Automation*, pages 671–676, 2016.
- [23] M. Bisgaard, A. Cour-Harbo, and J. D. Bendtsen. Adaptive control system for autonomous helicopter slung load operations. *Control Engineering Practice*, 18(7):800 – 811, 2010. Special Issue on Aerial Robotics.
- [24] S. Dai, T. Lee, and D. S. Bernstein. Adaptive control of a quadrotor UAV transporting a cable-suspended load with unknown mass. In *Conference on Decision and Control*, pages 6149–6154. IEEE, 2014.

- [25] M. Hua, T. Hamel, P. Morin, and C. Samson. Introduction to feedback control of underactuated VTOL vehicles: A review of basic control design ideas and principles. *Control Systems*, 33(1):61–75, 2013.
- [26] P. O. Pereira and D. V. Dimarogonas. Lyapunov-based generic controller design for thrust-propelled underactuated systems. In *European Control Conference*, pages 594–599, 2016.